

# Role of Radiomic Tissue Analysis in PET/CT in Mediastinal Lymphadenopathy in Extrathoracic and Lung Malignancies

## Ekstratorasik ve Akciğer Malignitelerinde Mediastinal Lenfadenopatide PET/BT'de Radyomik Doku Analizinin Rolü

 <sup>1</sup>Nurşin AGÜLOĞLU  
 <sup>2</sup>Ayşegül AKSU  
 <sup>3</sup>Damla SERÇE UNAT  
 <sup>4</sup>Onur Fevzi ERER  
 <sup>1</sup>Tuğçe ÇİFTÇİ DOKSÖZ

<sup>1</sup>Department of Nuclear Medicine, University of Health Sciences, İzmir Dr. Suat Seren Chest Diseases and Surgery Training and Research Hospital, İzmir, Türkiye

<sup>2</sup>Department of Nuclear Medicine, İzmir Katip Çelebi University, Atatürk Training and Research Hospital, İzmir, Türkiye

<sup>3</sup>Department of Chest Diseases, Kemalpaşa State Hospital, İzmir, Türkiye

<sup>4</sup>Department of Chest Diseases, Tinaztepe University Faculty of Medicine, Galen Hospital Chest Diseases, İzmir, Türkiye

### ABSTRACT

**Objective:** The objective of this study was to determine the metastasis status noninvasively by PET radiomic analysis of mediastinal and hilar lymph nodes (LN) detected by Fluor-18-fluorodeoxyglucose positron emission tomography/computed tomography (<sup>18</sup>F-FDG PET/CT) in patients with lung and extrathoracic malignancies.

**Material and Methods:** Images of 79 patients with mediastinal lymphadenopathy with lung and/or extrathoracic malignancy, who had undergone <sup>18</sup>F-FDG PET/CT imaging between January 2015 and July 2022, were evaluated using LIFEx software. The volume of interest (VOI) of the LNs was generated and volumetric and textural features were obtained from this VOI. Predictive analysis of benign and malign LNs was performed with these parameters.

**Results:** Significant differences were obtained between benign and malignant groups in all standard uptake value parameters, metabolic tumor volume (MTV), 2 shapes, and 28 tissue feature parameters. When SHAPesphericity, GLCMenergy, and MTV were evaluated by multivariate analysis, SHAPesphericity and GLCMenergy were obtained as the best features to distinguish benign and malignant groups ( $p < 0.001$ , OR: 1920.061, 43.425–84895.821, 95% CI and  $p = 0.009$ , OR: 0.001, 0.000–0.188, 95% CI). The sensitivity and specificity values of the model created with these two features in distinguishing the benign group were calculated as 90.1% and 56.8%, respectively (AUC: 0.742). There was a significant difference between the groups with extrapulmonary malignancy metastasis and benign ones in two shapes and one tissue analysis.

**Conclusion:** We think that the use of PET radiomic data will contribute to mediastinal and hilar LN staging in extrathoracic and/or lung cancer.

**Keywords:** <sup>18</sup>F-FDG PET/CT, extrathoracic malignancy, lung cancer, texture analysis.

**Cite this article as:** Ağuloğlu N, Aksu A, Serçe Unat D, Erer OF, Çiftçi Doksöz T. Role of Radiomic Tissue Analysis in PET/CT in Mediastinal Lymphadenopathy in Extrathoracic and Lung Malignancies. Journal of Izmir Chest Hospital 2022;36(3):141–147.

**Received (Geliş):** October 10, 2022 **Accepted (Kabul):** November 27, 2022 **Online (Çevrimiçi):** December 20, 2022

**Correspondence author (Sorumlu yazar):** Nurşin AGÜLOĞLU, MD. Sağlık Bilimleri Üniversitesi, İzmir Dr. Suat Seren Göğüs Hastalıkları ve Cerrahisi Eğitim Araştırma Hastanesi, Nükleer Tıp Bölümü, İzmir, Türkiye.

**Tel:** +90 232 433 33 33 **e-mail:** aguloglunursin@gmail.com

© Copyright 2022 by Journal of Izmir Chest Hospital - Available online at www.ighdergisi.org

**ORCID ID**

NA : 0000-0003-3976-2064

AA : 0000-0002-6239-0660

DSU : 0000-0003-4743-5469

OFE : 0000-0003-0509-0722

TÇD : 0000-0003-1282-3146

**ÖZ**

**Amaç:** Çalışmanın amacı, akciğer ve ekstratorasik malignitesi olan hastalarda, flor-18-florodeoksi glukoz pozitron emisyon tomografisi/bilgisayarlı tomografi (<sup>18</sup>F-FDG PET/BT) tarafından saptanan mediastinal ve hiler lenf nodlarının PET radyomik analizi ile noninvaziv olarak metastaz durumunu belirlemektir.

**Gereç ve Yöntemler:** Ocak 2015-Temmuz 2022 tarihleri arasında akciğer veya ekstratorasik malignitesi tespit edilen mediastinal lenfadenopatisi olan, <sup>18</sup>F-FDG PET/BT görüntülemesi yapılan 79 hastanın görüntüleri LIFEx yazılımı kullanılarak değerlendirildi. Lenf nodlarının ilgi hacmi (VOI) oluşturuldu ve bu VOI'dan hacimsel ve dokusal özellikler elde edildi. Bu parametreler ile lenf nodlarının malign-benign tahmin analizi yapıldı.

**Bulgular:** Benign ve malign gruplar arasında tüm standart alım değeri (SUV) parametrelerinde, metabolik tümör hacmi (MTV)'de, iki şekil, 28 doku özelliği parametrelerinde anlamlı farklılıklar elde edildi. SHAPESphericity, GLCMenergy ve MTV, çok değişkenli analizle değerlendirildiğinde, SHAPESphericity ve GLCMenergy, benign ve malign grupları ayırmada en iyi özellikler olarak elde edildi ( $p < 0,001$ , OR: 1920,061, 43,425–84895,821, %95 CI ve  $p = 0,009$ , OR: 0,001, 0,000–0,188, %95 CI). Bu iki özellikle oluşturulan modelin benign grubu ayırt etmedeki duyarlılık ve özgüllük değerleri sırasıyla %90,1 ve %56,8 olarak hesaplandı (AUC: 0,742). Akciğer dışı malignite metastazı olan ve benign saptanan gruplar arasında iki şekil, bir doku analizi özelliğinde anlamlı farklılık saptandı.

**Sonuç:** PET radyomik verilerin kullanımının, ekstratorasik ve/veya akciğer kanserinde mediastinal ve hiler lenf nodu evrelemesi için katkı sağlayacağını düşünmekteyiz.

**Anahtar kelimeler:** Flor-18-florodeoksi glukoz, ekstratorasik malignite, akciğer kanseri, doku analizi.

**INTRODUCTION**

Mediastinal lymph node (LN) enlargement has many causes, including infectious, malignant, and inflammatory conditions.<sup>[1]</sup> Mediastinal lymphadenopathy is a common finding in patients with lung or extrathoracic malignancies. The presence of mediastinal lymphadenopathies has an important role in staging the disease, planning the treatment, and evaluating the prognosis. In patients with malignancy, mediastinal or hilar LN enlargement may also be due to tuberculosis, granulomatous inflammation, and reactive changes, apart from malignant causes.<sup>[2,3]</sup>

Positron emission tomography/computed tomography (PET/CT) is very important for the evaluation of mediastinal or hilar lesions and appropriate treatment planning in patients with non-small cell lung cancer (NSCLC). However, the distinction between malignant and benign lesions cannot be made precisely with this method. The positive predictive value in the evaluation of LN involvement with PET/CT has been accepted at a rate ranging from 32.3% to 89%.<sup>[4–6]</sup> FDG-PET/CT is a method that helps guide invasive staging methods such as endobronchial ultrasound-guided transbronchial needle aspiration/biopsy (EBUS-TBNA) and constitutes the first step of this study. Mediastinal LN metastasis is also seen in extrathoracic malignancies, and PET/CT is used to detect metastases. In a study evaluating the role of EBUS imaging and PET/CT scanning, the most common extrathoracic carcinomas that metastasize to the mediastinum were colorectal, breast, stomach, head and neck, and urogenital carcinomas.<sup>[7]</sup>

PET/CT-based radiomic analysis is a branch of research that expresses quantitative data obtained from medical imaging and analyzed by mathematical methods. Predictive models developed with radiomic data can play a role in oncological diagnosis and treatment guidance, thus can support personalized treatment. In texture analysis, data are obtained according to the gray level densities of the voxels in the image and the distribution of these densities. Quantitative radiomic approach obtained from <sup>18</sup>F-FDG PET/CT images has taken its place in research as a non-invasive method for determining tumor phenotype. Several studies have suggested that tissue analysis has predictive value in diagnostic imaging in different types of cancer.<sup>[8–11]</sup>

There are studies, in which mediastinal LNs were evaluated with PET radiomic analysis in benign and lung malignant groups.<sup>[12,13]</sup> However, to the best of our knowledge, there is no study evaluating mediastinal LN metastases of extrathoracic malignancies by radiomic analysis. Therefore, in this study, it was aimed to non-invasively determine the metastasis status by PET radiomic analysis of mediastinal and/or hilar LNs detected by PET/CT in patients with lung and/or extrathoracic malignancies.

**MATERIAL AND METHODS****Patient Selection**

The files of patients who were diagnosed with lung and/or extrathoracic malignancies in our hospital and who underwent <sup>18</sup>F-FDG PET/CT imaging between January 2015 and July 2022 were retrospec-

tively analyzed. The inclusion criteria of the patients were as follows: (1). Histopathological diagnosis of extrathoracic or lung malignancy, (2). those with endobronchial ultrasound-guided transbronchial needle aspirate (EBUS-TBNA) biopsy data of mediastinal and/or hilar lymphadenopathies, (3). time between PET/CT scan and EBUS-TBNA being <3 weeks, and (4). segmented area being over 64 voxels. The exclusion criteria were as follows: (1). Poor quality images (poor images due to noise, respiratory artifacts or other motion artifacts, and missing PET images or CT images), (2). LN involvement below mediastinal background activity, (3). PET/CT images of LNs with indistinguishable borders from the primary mass lesion, and (4). LNs with a short axis diameter below 5 mm. LNs with a pathology of reactive and granulomatous were included in the “benign” group, and those with metastatic disease were included in the “malignant” group. In the study, mediastinal lymphadenopathies of colon, ovarian, and stomach cancers, which are extrathoracic malignancies, were evaluated.

In our study, permission was obtained from our Institutional Ethics Committee for the use of patient data for publication in accordance with the local clinical practice guidelines and applicable legislation (Approval number: 2022/42-46).

### PET/CT Protocol

Imaging was performed in a Philips Gemini TF 16-slice combined PET/CT scanner, with the same scanner used for all patients. Following a minimum of 6 h of fasting (blood glucose concentrations <150 ng/dl), 8–15 mCi  $^{18}\text{F}$ -FDG (2.5 MBq/kg body weight) was administered intravenously in accordance with European Nuclear Medicine Association guidelines version 2.0.<sup>[14]</sup> The time between intravenous injection and scans was  $60\pm 5$  min. First, CT images (140 kV, 100 mAs, 5 mm sections) were obtained without using contrast. PET images were then acquired through whole-body scanning from the skull apex to the proximal thigh, using 1.5 min of emission scanning per bed position and 9 or 10 bed positions (Philips Gemini TF; Philips). Attenuation correction was performed with obtained CT images. The voxel size was  $4\times 4\times 4$  mm. Images were reconstructed with row action maximum likelihood algorithm.

### $^{18}\text{F}$ -FDG PET/CT Texture Analysis

The images of the patients were evaluated using the semi-automatic LIFEx (LIFEx, Orsay, France) software.<sup>[15]</sup> PET/CT image of the patient in DICOM format was transferred to the software. The relevant region of the target lesion was evaluated semi-automatically by a nuclear medicine physician with 10 years of PET/CT experience using a 41% maximum standardized uptake value ( $\text{SUV}_{\text{max}}$ ) threshold value in  $^{18}\text{F}$ -FDG PET/CT hybrid images (Fig. 1). Conventional SUV parameters, volumetric, histogram, and shape parameters were obtained. In further textural analysis, gray-level co-occurrence matrix (GLCM), gray-level run length matrix (GLRLM), neighborhood gray-level different matrix (NGLDM), and gray-level zone length matrix parameters were measured. These features are summarized in Table 1.

### Statistical Analysis

The Statistical Package for the Social Sciences (SPSS) v. 22.0 was used for the statistical analysis. p value of <0.05 was considered significant. Normally distributed data were presented as

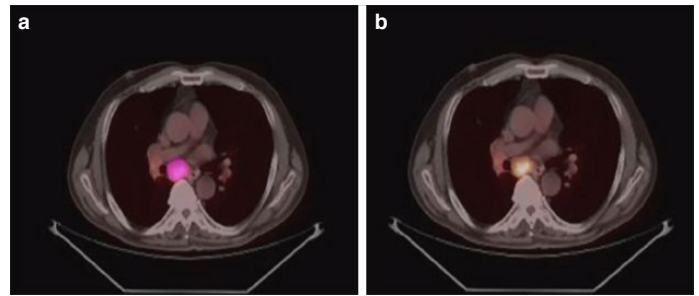


**Figure 1:** (a) Segmentation (with pink color), (b) PET/CT fusion image of the mediastinal lymph node in the  $^{18}\text{F}$ -FDG PET/CT with LIFEx software.

$^{18}\text{F}$ -FDG PET/CT: Fluor-18-fluorodeoxyglucose positron emission tomography/computed tomography.

mean $\pm$ standard deviation, and non-normal distributed data were given as median (range). The correlation between features was evaluated by Spearman correlation analysis. The differences between age, SUV, volumetric and texture analysis parameters between two groups were analyzed by the Mann-Whitney U-test. The relationship between categorical variables was evaluated by Chi-square or Fisher exact tests. The features with a correlation coefficient of less than 0.6 were analyzed with logistic regression; the others were not included in the further analysis. A model was created with radiomic features. The model performance was evaluated by area under curve (AUC) obtained from the receiver operating characteristic analysis. The sensitivity and specificity values of the models were calculated.

### RESULTS

Of 79 patients with lung and/or extrathoracic malignancies, 30 (38%) were female, 49 (62%) were male, and the mean age was  $63\pm 12$  years. One hundred and seventy-five lymphadenopathies were detected in these patients. Twenty-seven (15.4%) LNs were concluded as extrapulmonary malignancy metastases, 47 (26.9%) LNs as lung ca metastases, 57 (32.6%) LNs as granulomatous pathologies, and 44 (25.1%) LNs as reactive changes. While there were 101 LNs in the benign group, 74 LNs were found to be metastatic.

There was no relationship between benign and malignant groups and gender ( $p=0.788$ ). There was no significant difference in patient ages between the benign and malignant groups ( $p=0.320$ ).

Significant differences were obtained between benign and malignant groups in all SUV parameters, metabolic tumor volume (MTV), two shapes, and 28 tissue feature parameters. When the correlations of these parameters with each other were analyzed, it was seen that the correlation coefficients of SHAPesphericity, GLCMenergy, and MTV were below 0.6.

When SHAPesphericity, GLCMenergy, and MTV were evaluated by multivariate analysis, SHAPesphericity and GLCMenergy were obtained as the best features for discriminating benign from malignant groups ( $p<0.001$ , OR: 1920.061, 43.425–84895.821, 95% CI and  $p=0.009$ , OR: 0.001, 0.000–0.188, 95% CI). The sensitivity and specificity values of the model created with these two features in distinguishing the benign group were calculated as 90.1% and 56.8%, respectively (AUC: 0.742) (Table 2).

**Table 1: Definition of parameters evaluated including conventional and advanced metabolic indices, shape features, and radiomic texture features**

Index	Matrix	Parameter
Conventional indices		SUV <sub>min</sub> , SUV <sub>mean</sub> , and SUV <sub>max</sub> , SUV <sub>peak</sub> and SUV <sub>Std</sub>
Volumetric indices		MTV and TLG
Radiomic Texture features	GLCM	Homogeneity, energy, contrast, correlation, entropy, and dissimilarity
	NGLDM	Coarseness, contrast, and busyness
	GLRLM	SRE, LRE, LGRE, HGRE, SRLGE, SRHGE, LRLGE, LRHGE, GLNU, RLNU, and RP
	GLZLM	SZE, LZE, LGZE, HGZE, SZLGE, SZHGE, LZLGE, LZHGE, GLNU, ZLNU, and ZP
Shape features		Sphericity, surface, and compacity

SUV: Standard uptake value, MTV: Metabolic tumor volume, TLG: Total lesion glycolysis, GLCM: Gray-level co-occurrence matrix, NGLDM: Neighborhood gray-level diferent matrix, GLRLM: Gray-level run-length matrix, GLZLM: Graylevel zone-length matrix, SRE: Short-run emphasis, LRE: Long-run emphasis, LGRE: Low gray-level run emphasis, HGRE: High gray-level run emphasis, SRLGE: Short-run low gray-level emphasis, SRGHE: Short-run high gray-level emphasis, LRLGE: Long-run row gray-level emphasis, LRHGE: Long-run high gray-level emphasis, GLNU: Gray-level non-uniformity, RLNU: Run-length non-uniformity, RP: Run percentage, SZE: Short-zone emphasis, LZE: Long-zone emphasis, LGZE: Low gray-level zone emphasis, HGZE: High gray-level zone emphasis, SZLGE: Short-zone low gray-level emphasis, SZHGE: Short-zone high gray-level emphasis, LZLGE: Long-zone low gray-level emphasis, LZHGE: long-zone high gray-level emphasis, ZLNU: Zone-length non-uniformity, ZP: Zone percentage.

**Table 2: Analysis of SUV, volumetric, and tissue properties between malignant and benign groups**

Feature	p	AUC	CI 95%	Feature	p	AUC	CI 95%
SUV <sub>min</sub>	0.001	0.641	0.558–0.723	GLRLM SRLGE	0.001	0.643	0.561–0.726
SUV <sub>mean</sub>	0.001	0.646	0.564–0.728	GLRLM SRHGE	0.001	0.644	0.562–0.726
SUV <sub>std</sub>	0.001	0.649	0.567–0.731	GLRLM LRLGE	0.001	0.645	0.563–0.728
SUV <sub>max</sub>	0.001	0.641	0.559–0.724	GLRLM LRHGE	0.001	0.644	0.562–0.726
SUV <sub>peak</sub>	0.001	0.648	0.566–0.729	GLRLM GLNU	0.001	0.652	0.571–0.734
TLG	0.697	–	–	GLRLM RLNU	0.765	–	–
MTV	0.021	0.603	0.518–0.687	GLRLM RP	0.002	0.638	0.555–0.720
SHAPEsphericity	<0.001	0.704	0.625–0.783	NGLDMcoarseness	0.030	0.596	0.512–0.681
SHAPEsurface	0.002	0.638	0.555–0.721	NGLDMcontrast	0.002	0.640	0.557–0.722
SHAPEcompacity	0.497	–	–	NGLDMbusyness	<0.001	0.656	0.575–0.737
GLCMhomogeneity	<0.001	0.659	0.577–0.740	GLZLM SZE	0.041	0.591	0.504–0.677
GLCMenergy	<0.001	0.671	0.591–0.752	GLZLM LZE	0.002	0.638	0.556–0.720
GLCMcontrast	0.001	0.648	0.565–0.730	GLZLM LGZE	0.003	0.630	0.546–0.715
GLCMcorrelation	0.365	–	–	GLZLM HGZE	0.003	0.631	0.547–0.715
GLCMentropylog10	<0.001	0.669	0.589–0.749	GLZLM SZLGE	0.022	0.601	0.517–0.686
GLCMdissimilarity	<0.001	0.651	0.569–0.732	GLZLM SZHGE	0.009	0.616	0.531–0.701
GLRLM SRE	0.002	0.637	0.555–0.720	GLZLM LZLGE	0.001	0.641	0.559–0.724
GLRLM LRE	0.001	0.642	0.560–0.724	GLZLM LZHGE	0.039	0.592	0.508–0.675
GLRLM LGRE	0.001	0.644	0.561–0.726	GLZLM GLNU	0.392	–	–
GLRLM HGRE	0.001	0.646	0.564–0.728	GLZLM ZLNU	0.010	0.614	0.530–0.697
				GLZLM ZP	0.003	0.633	0.550–0.715

AUC: Area under curve, CI: Confidence interval.

A significant difference was found between the groups with extrapulmonary malignancy metastasis (n=27) and benign groups in terms of two shapes and one tissue analysis. The correlation coefficients of SHAPEsphericity and GLCMcorrelation features were below 0.6 (Table 3).

Significant differences were found between the malignant (n=75) and granulomatous (n=56) groups in SUVstd, MTV, two shapes, and four tissue characteristic parameters (Table 4).

The correlation matrix of significant and non-significant radiomic features is shown in Figure 2.

**Table 3: Extrathoracic metastatic and benign lymph nodes analysis**

Feature	p	AUC	CI 95%
SHAPEsphericity	<0.001	0.784	0.693–0.874
SHAPEsurface	0.003	0.688	0.577–0.798
GLCMcorrelation	0.047	0.625	0.508–0.742

AUC: Area under curve, CI: Confidence interval. GLCM: Gray-level co-occurrence matrix.

## DISCUSSION

In our study, we investigated that the role of metabolic, volumetric, and textural features obtained from <sup>18</sup>F-FDG PET/CT images in predicting the discrimination of malignant from benign mediastinal LNs. In this direction, we have shown that PET/CT imaging and tissue analysis parameters can contribute to benign-malignant discrimination without the need for invasive procedures under necessary conditions. Among the benign and malignant groups, SHAPEsphericity and GLCMenergy were obtained as the best features in distinguishing the benign and malignant groups. The sensitivity and specificity values of the model created with these two features in distinguishing the benign group were calculated as 90.1% and 56.8%, respectively (AUC: 0.742). We think that it may be effective in determining the status of the mediastinal LN and the treatment management of the patients in extrathoracic and lung malignancies.

False positivity of mediastinal LNs is common in functional imaging with <sup>18</sup>F-FDG PET/CT. Because this modality is considered positive due to infection, inflammation, or inflammation due to granulomatous diseases.<sup>[16–18]</sup> The mechanism of high FDG uptake in benign mediastinal LNs is glucose transporter-1 overexpression associated with lymphoid follicular hyperplasia and histiocyte infiltration.<sup>[19]</sup> Benign mediastinal LNs might appear as a false-positive finding on PET imaging, and lower FDG uptake may be metastatic and increase the risk of misdiagnosis. Therefore, distinction between malignant and benign extrathoracic and lung malignancies in mediastinal LNs is of utmost importance in accurate diagnosis and staging, treatment planning, detection of recurrences, and determination of prognosis.

Kandemir et al.<sup>[20]</sup> determined the cutoff value for SUV<sub>max</sub> as 6.3 in distinguishing the presence of LN metastasis in 31 patients with lung and extrathoracic malignancies and reported the sensitivity and specificity at this cutoff value as 70.6% and 83.3%, respectively. Lee et al.<sup>[21]</sup> determined the cutoff as 5.3 for SUV<sub>max</sub> in detecting LN metastasis in 110 patients with NSCLC and found the sensitivity to be 81% and the specificity to be 98%. However, in these studies, SUV<sub>max</sub> parameter obtained from a single voxel was used. The intensity of FDG uptake may differ both in different tumor types and subtypes. For example, Cuaron et al.<sup>[22]</sup> found that squamous cell carcinomas showed more FDG uptake than adenocarcinomas and reported that different subtypes differed in terms of <sup>18</sup>F-FDG uptake. This finding is mainly attributed to differences in the expression of the glucose transporter.<sup>[23]</sup> Flechsig et al.<sup>[24]</sup> also could not confirm mediastinal and hilar LN metastases, according to the level of FDG uptake in LN metastases.

**Table 4: SUV, volumetric, and tissue characteristics analysis of malignant and granulomatous lymph nodes**

Feature	p	AUC	CI 95%
SUV <sub>min</sub>	0.076	–	–
SUV <sub>mean</sub>	0.069	–	–
SUV <sub>std</sub>	0.040	0.605	0.506–0.704
SUV <sub>max</sub>	0.073	–	–
SUV <sub>peak</sub>	0.060	–	–
TLG	0.114	–	–
MTV	0.006	0.640	0.543–0.738
SHAPEsphericity	<0.001	0.752	0.669–0.835
SHAPEsurface	<0.001	0.680	0.586–0.774
SHAPEcompactness	0.642	–	–
GLCMhomogeneity	0.112	–	–
GLCMenergy	0.073	–	–
GLCMcontrast	0.079	–	–
GLCMcorrelation	0.232	–	–
GLCMentropylog10	0.076	–	–
GLCMdissimilarity	0.097	–	–
GLRLM SRE	0.255	–	–
GLRLM LRE	0.216	–	–
GLRLM LGRE	0.075	–	–
GLRLM HGRE	0.063	–	–
GLRLM SRLGE	0.072	–	–
GLRLM SRHGE	0.065	–	–
GLRLM LRLGE	0.068	–	–
GLRLM LRHGE	0.057	–	–
GLRLM GLNU	0.006	0.642	0.545–0.739
GLRLM RLNU	0.024	–	–
GLRLM RP	0.263	–	–
NGLDMcoarseness	0.003	0.654	0.559–0.750
NGLDMcontrast	0.104	–	–
NGLDMbusyness	0.005	0.643	0.546–0.740
GLZLM SZE	0.560	–	–
GLZLM LZE	0.141	–	–
GLZLM LGZE	0.058	–	–
GLZLM HGZE	0.061	–	–
GLZLM SZLGE	0.011	0.631	0.534–0.728
GLZLM SZHGE	0.161	–	–
GLZLM LZLGE	0.101	–	–
GLZLM LZHGE	0.484	–	–
GLZLM GLNU	0.083	–	–
GLZLM ZLNU	0.655	–	–
GLZLM ZP	0.219	–	–

AUC: Area under curve, CI: Confidence interval.

Therefore, going beyond maximum SUV use and evaluating the entire lesion will give more accurate results. On the other hand, we wanted to investigate the contribution of radiomic analysis,

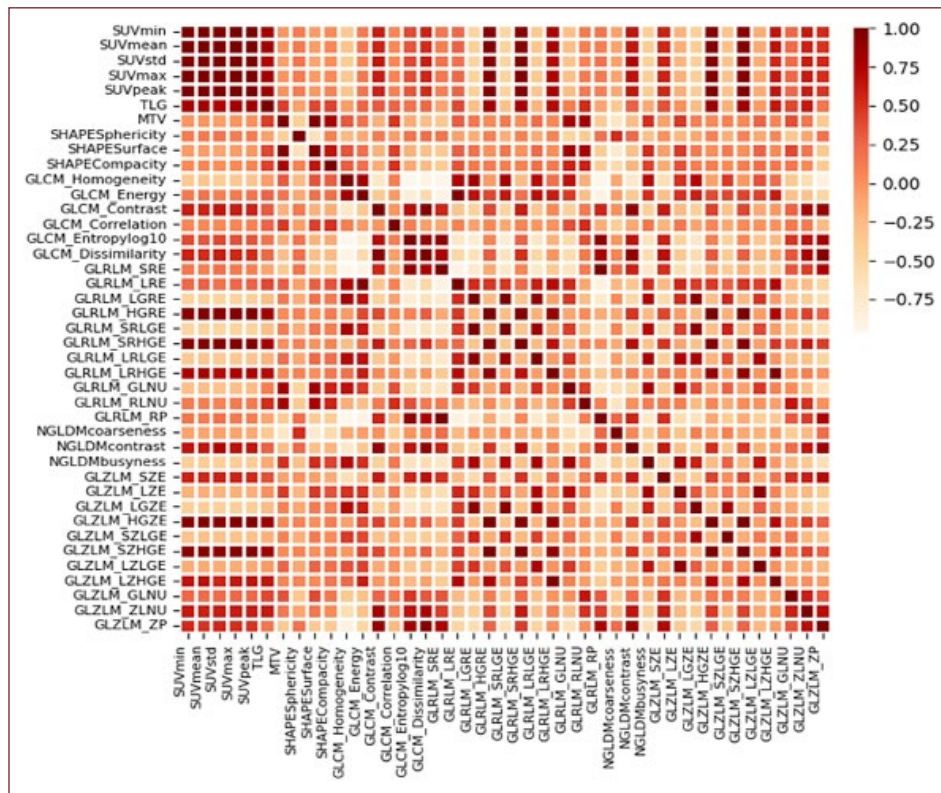


Figure 2: Correlation matrix of obtained radiomic features.

which has been developing in recent years and enables non-invasive evaluation of the heterogeneity of the lesion from imaging modalities, in detecting LN metastasis, and our results gave rise to the thoughts that evaluating the heterogeneity of LNs may have an important place in predicting the presence of metastasis. In our study, SHAPESphericity and GLCMenergy were obtained as the best features in separating benign and malignant groups. These tissue features represent the heterogeneity and homogeneity of the LNs. There are several studies in the literature using radiomic analysis to detect metastatic LNs in patients with lung cancer. In the study of Hoshino et al.<sup>[25]</sup> GLRLM\_GLNU, GLRLM\_RLNU, and NGLDM\_Coarseness were found to differ between true and false positives of the LNM groups; this showed that metastatic LNs in patients with esophageal cancer showed higher tissue heterogeneity than non-metastatic LNs. Ouyang et al.<sup>[13]</sup> also detected significant differences in DISCRETIZED\_HISTO\_ExcessKurtosis, GLRLM\_GLNU, GLRLM\_RLNU, and NGLDM\_Coarseness features in detecting metastatic LNs in lung cancers. In addition to these studies, we included patients with extrathoracic malignancies in our study so that we could evaluate metastatic LNs in the mediastinal region as a large group.

In our study, we noticed that SHAPESphericity was the most successful feature in the discrimination of benign from malignant, malignant from granulomatous LN, and extrathoracic metastasis from benign LN. Benign LNs were more spherical than malignant LNs, and asphericity was more prominent in malignant LNs. The aspheric appearance of the lesion is an indicator of heterogeneity and is an important parameter in both diagnosis and prognosis prediction. In

this regard, Apostolava et al.<sup>[26]</sup> 52 found that asphericity in the primary tumor before treatment was an important prognostic indicator in predicting tumor progression and survival. These results support the result obtained in our study.

Kim et al.<sup>[27]</sup> showed that  $SUV_{max}$  and MTV determined by  $^{18}F$ -FDG PET/CT were statistically significant predictors in patients with cN0 NSCLC. Similarly, in our study, a significant difference was found in SUV parameters and MTV between malignant and benign groups. In addition, when we compared LNs only in the granulomatous group with metastatic LNs, we found significant differences in SUV, MTV, and some shape and tissue characteristics.

Our study contains a small sample size and has limitations due to its retrospective design. Multicenter studies with a large patient population are needed for further validation. In this context, standardization of methodology and harmonization of radiomic results will become more important in later studies. It is necessary to use and reproduce these methods because they are required to be used as predictors of clinical outcomes.

### CONCLUSION

We think that the use of PET radiomic data will contribute to mediastinal and hilar LN staging in extrathoracic and lung cancer. Evaluation of the heterogeneity of the lymph node in a non-invasive way will enable patients to waste less time and contribute to the process of diagnosis, follow-up, treatment, and evaluation of response to treatment in precision medicine.

## Disclosures

**Ethics Committee Approval:** The study was approved by The University of Health Sciences, İzmir Dr. Suat Seren Chest Diseases and Surgery Training and Research Hospital Clinical Research Ethics Committee (date: 08.06.2022, number: 2022/42-46).

**Peer-review:** Externally peer-reviewed.

**Author Contributions:** Concept – N.A.; Design – N.A.; Supervision – N.A., A.A.; Fundings – None; Materials – N.A., O.F.E., T.Ç.D.; Data Collection and/or Processing – N.A., O.F.E., T.Ç.D.; Analysis and/or Interpretation – N.A., A.A.; Literature Search – N.A., D.S.U.; Writing – N.A., A.A.; Critical Reviews – N.A., A.A.

**Conflict of Interest:** The authors have no conflict of interest to declare.

**Financial Disclosure:** The authors declared that this study has received no financial support.

## REFERENCES

- Evison M, Crosbie PA, Morris J, Martin J, Barber PV, Booton R. A study of patients with isolated mediastinal and hilar lymphadenopathy undergoing EBUS-TBNA. *BMJ Open Respir Res* 2014;1:e000040.
- Yang B, Li F, Shi W, Liu H, Sun S, Zhang G, et al. Endobronchial ultrasound-guided transbronchial needle biopsy for the diagnosis of intrathoracic lymph node metastases from extrathoracic malignancies: A meta-analysis and systematic review. *Respirology* 2014;19:834–41.
- Ercan S, Nichols FC 3<sup>rd</sup>, Trastek VF, Deschamps C, Allen MS, Miller DL, et al. Prognostic significance of lymph node metastasis found during pulmonary metastasectomy for extrapulmonary carcinoma. *Ann Thorac Surg* 2004;77:1786–91.
- Antoch G, Stattaus J, Nemat AT, Marnitz S, Beyer T, Kuehl H, et al. Non-small cell lung cancer: Dual-modality PET/CT in preoperative staging. *Radiology* 2003;229:526–33.
- Lin WY, Hsu WH, Lin KH, Wang SJ. Role of preoperative PET-CT in assessing mediastinal and hilar lymph node status in early stage lung cancer. *J Chin Med Assoc* 2012;75:203–8.
- Perigaud C, Bridji B, Roussel JC, Sagan C, Mugniot A, Duveau D, et al. Prospective preoperative mediastinal lymph node staging by integrated positron emission tomography-computerised tomography in patients with non-small-cell lung cancer. *Eur J Cardiothorac Surg* 2009;36:731–6.
- Song JU, Park HY, Jeon K, Koh WJ, Suh GY, Chung MP, et al. The role of endobronchial ultrasound-guided transbronchial needle aspiration in the diagnosis of mediastinal and hilar lymph node metastases in patients with extrapulmonary malignancy. *Intern Med* 2011;50:2525–32.
- Coroller TP, Agrawal V, Huynh E, Narayan V, Lee SW, Mak RH, et al. Radiomic-Based pathological response prediction from primary tumors and lymph nodes in NSCLC. *J Thorac Oncol* 2017;12:467–76.
- Orlhac F, Soussan M, Maisonobe JA, Garcia CA, Vanderlinden B, Buvat I. Tumor texture analysis in <sup>18</sup>F-FDG PET: Relationships between texture parameters, histogram indices, standardized uptake values, metabolic volumes, and total lesion glycolysis. *J Nucl Med* 2014;55:414–22.
- Hatt M, Majdoub M, Vallières M, Tixier F, Le Rest CC, Groheux D, et al. <sup>18</sup>F-FDG PET uptake characterization through texture analysis: Investigating the complementary nature of heterogeneity and functional tumor volume in a multi-cancer site patient cohort. *J Nucl Med* 2015;56:38–44.
- van Rossum PS, Fried DV, Zhang L, Hofstetter WL, van Vulpen M, Meijer GJ, et al. The incremental value of subjective and quantitative assessment of <sup>18</sup>F-FDG PET for the prediction of pathologic complete response to preoperative chemoradiotherapy in esophageal cancer. *J Nucl Med* 2016;57:691–700.
- Zheng K, Wang X, Jiang C, Tang Y, Fang Z, Hou J, et al. Pre-Operative prediction of mediastinal node metastasis using radiomics model based on <sup>18</sup>F-FDG PET/CT of the primary tumor in non-small cell lung cancer patients. *Front Med (Lausanne)* 2021;8:673876.
- Ouyang ML, Wang YR, Deng QS, Zhu YF, Zhao ZH, Wang L, et al. Development and validation of a <sup>18</sup>F-FDG PET-Based radiomic model for evaluating hypermetabolic mediastinal-hilar lymph nodes in non-small-cell lung cancer. *Front Oncol* 2021;11:710909.
- Boellaard R, Delgado-Bolton R, Oyen WJ, Giammarile F, Tatsch K, Eschner W, et al. FDG PET/CT: EANM procedure guidelines for tumour imaging: Version 2.0. *Eur J Nucl Med Mol Imaging* 2015;42:328–54.
- Nioche C, Orhac F, Boughdad S, Reuzé S, Goya-Outi J, Robert C, et al. LIFEX: A freeware for radiomic feature calculation in multimodality imaging to accelerate advances in the characterization of tumor heterogeneity. *Cancer Res* 2018;78:4786–9.
- Kang F, Wang S, Tian F, Zhao M, Zhang M, Wang Z, et al. Comparing the diagnostic potential of <sup>68</sup>Ga-Alfamide II and <sup>18</sup>F-FDG in differentiating between non-small cell lung cancer and tuberculosis. *J Nucl Med* 2016;57:672–7.
- Choi EK, Park HL, Yoo IR, Kim SJ, Kim YK. The clinical value of F-<sup>18</sup>FDG PET/CT in differentiating malignant from benign lesions in pneumoconiosis patients. *Eur Radiol* 2020;30:442–51.
- Flechsip P, Kratochwil C, Schwartz LH, Rath D, Moltz J, Antoch G, et al. Quantitative volumetric CT-histogram analysis in N-staging of <sup>18</sup>F-FDG-equivocal patients with lung cancer. *J Nucl Med* 2014;55:559–64.
- Kwon SY, Min JJ, Song HC, Choi C, Na KJ, Bom HS. Impact of lymphoid follicles and histiocytes on the false-positive FDG uptake of lymph nodes in non-small cell lung cancer. *Nucl Med Mol Imaging* 2011;45:185–91.
- Kandemir Z, Sentürk A, Ozdemir E, Yildirim N, Hasanoğlu HC, Keskin M, et al. The evaluation of hypermetabolic mediastinal-hilar lymph nodes determined by PET/CT in pulmonary and extrapulmonary malignancies: Correlation with EBUS-TBNA. *Turk J Med Sci* 2015;45:1234–42.
- Lee BE, Redwine J, Foster C, Abella E, Lown T, Lau D, et al. Mediastinoscopy might not be necessary in patients with non-small cell lung cancer with mediastinal lymph nodes having a maximum standardized uptake value of less than 5.3. *J Thorac Cardiovasc Surg* 2008;135:615–9.
- Cuaron J, Dunphy M, Rimner A. Role of FDG-PET scans in staging, response assessment, and follow-up care for non-small cell lung cancer. *Front Oncol* 2013;2:208.
- Brown RS, Leung JY, Kison PV, Zasadny KR, Flint A, Wahl RL. Glucose transporters and FDG uptake in untreated primary human non-small cell lung cancer. *J Nucl Med* 1999;40:556–65.
- Flechsip P, Frank P, Kratochwil C, Antoch G, Rath D, Moltz J, et al. Radiomic analysis using density threshold for FDG-PET/CT-Based N-staging in lung cancer patients. *Mol Imaging Biol* 2017;19:315–22.
- Hoshino I, Yokota H, Ishige F, Iwatate Y, Takeshita N, Nagase H, et al. Radiogenomics predicts the expression of microRNA-1246 in the serum of esophageal cancer patients. *Sci Rep* 2020;10:2532.
- Apostolova I, Steffen IG, Wedel F, Lougovski A, Marnitz S, Derlin T, et al. Asphericity of pretherapeutic tumour FDG uptake provides independent prognostic value in head-and-neck cancer. *Eur Radiol* 2014;24:2077–87.
- Kim DH, Song BI, Hong CM, Jeong SY, Lee SW, Lee J, et al. Metabolic parameters using <sup>18</sup>F-FDG PET/CT correlate with occult lymph node metastasis in squamous cell lung carcinoma. *Eur J Nucl Med Mol Imaging* 2014;41:2051–7.